Laser spectroscopic characterization of supersonic jet cooled 2,6-diazaindole (26DAI)

Bhavika Kalal,[a] Simran Baweja,[a] Surajit Maity[a,*]

[a]Department of Chemistry, IIT Hyderabad, Telangana, India, 502284

*surajitmaity@chy.iith.ac.in

Abstract: In this article, we present the laser spectroscopic investigation of a nitrogen rich indole derivative, 2,6-diazaindole (26DAI) in the gas phase for the first time. Laser induced fluorescence (LIF) and two-color resonant two-photon ionization (2C-R2PI) spectroscopies were carried out to understand the role of N-insertion on the electronic excitation of indole derivatives. The band origin for $S_1 \leftarrow S_0$ electronic transition was observed at 33915 cm^{-1}, which was red shifted by 713 cm^{-1} and 1317 cm^{-1} from that of 7-azaindole and indole, respectively. The single vibronic level fluorescence (SVLF) spectroscopy of the molecule depicted a large Franck-Condon activity till 2500 cm^{-1} for ground state vibrational modes. The experimental vibrational frequencies from the SVLF spectrum were compared to Franck-Condon simulated frequencies at two different level of theories. The more accurate results were found at B3LYP-D4/def2-TZVPP, than the more energy demanding MP2/cc-pVDZ level. Fluorescence-dip infrared (FDIR) spectrum was recorded to determine the N-H stretching frequency of the molecule in the ground state, which was observed at 3524 cm^{-1}. The photoionization efficiency spectroscopy was performed to measure the ionization energy of the molecule as 71866 cm^{-1}, which is significantly higher as compared to 7-azaindole and indole. Thus, the above study suggests that the N-rich biomolecules appear to have a considerably lower risk of photodamage. The current investigation can shed light on to the nature's way of stabilizing bio-relevant molecules with a possible N-insertion mechanism.

Keywords: Photo-stability, Electronic Spectroscopy, Laser Induced Fluorescence, IR-UV double resonance spectroscopy, Dispersed fluorescence spectroscopy

1. Introduction

Azaindoles constitute the central structure of numerous biologically active compounds. The N-rich indole derivatives, such as tryptophan, are the key motifs in many proteins which play important role in structure and properties of proteins.[1,2] In many biorelevant molecules, the indole moiety is responsible for their antioxidant potency.[3] Understanding the structure, photophysical characteristics and photo-stability have been a topic of immense interest among researchers.[4,5] Additionally, the N-containing aromatic molecules have demonstrated promising biological activities, including anticancer, antimicrobial, and anti-inflammatory properties, making them a critical target for pharmaceutical research in the field of drug discovery and development.[6–11] Their easily modifiable structure allows for the synthesis of a wide range of molecular structures with applications in organic chemistry, medicinal chemistry, and materials science. Azaindole and its metal complexes have been studied in development of novel catalysts, luminescent materials, and functionalized coordination polymers.[12–15] Therefore, investigations on the spectroscopic characteristics, photo-acidity and photo-stability of selective N-rich indole derivative is of great interest in chemistry, biology and pharmaceutical communities.

The most popular N-containing indole derivative, which was widely investigated in the literature is 7-Azaindole (7AI).[16] The molecule has been extensively studied as it has higher fluorescence lifetime compared to that of its biorelevant counterpart tryptophan.[17–23] The ionisation potential (I.P.) for indole molecule is 7.76 eV (62589 cm^{-1}) and for 7-azaindole, which has an additional N-atom, I.P. is 8.11 eV (65412 cm^{-1}).[24,25] Chou et al. reported that the 2,7-diazaindole (27DAI), a 7AI analogue with one additional N-atom, can show a better photophysical properties in the solution phase.[5] The ionisation potential of 27DAI is 8.921 eV (71953 cm^{-1}) in the gas phase, implying that the insertion of N-atom can increase the photostability of the such biorelevant molecules.[26] The photofragmentation study of three protonated azaindole molecules 7-azaindole, 6-azaindole, and 5-azaindole, has revealed that excited state lifetime is shorter in case of 5- and 6-azaindole compared to 7-azaindole suggesting that the position of the N atom in six membered ring of azaindole molecules plays an intrinsic role in the energies of higher electronic states and photofragmentation dynamics of the molecule.[27] Chou et al. have studied 2,6-diazaindole (26DAI), an analogue of 2,7-diazaindole (27DAI), in solvation phase to probe multi-proton transfer in aqueous solution.[28]

Theoretical studies of proton and hydrogen transfer reaction mechanism in 26DAI have also been performed.[29–31] There are no reports so far on the experimental investigations on 26DAI molecule, so starting this seminal research would be crucial from fundamental and practical standpoint.

Herein, we aim to experimentally determine the ground state and excited state properties of the 26DAI molecule in the supersonic jet cooled molecular beam produced in the gas phase. We have characterised the molecule using various laser spectroscopic techniques. The single vibronic level fluorescence (SVLF) spectroscopy was employed to investigate the ground state vibrational energy levels. Laser induced fluorescence (LIF) and two-color resonant two-photon ionization (2C-R2PI) spectroscopies are performed to obtain the $S_0 \rightarrow S_1$ band origin transition. The ground state N-H stretching frequency was determined using fluorescence dip infrared (FDIR) spectroscopy. The photo-stability of the molecule was characterized by measuring the photoionization efficiency (PIE) spectrum. The current experimental investigation is crucial to understand the effect of N-substitution on the photo-stability of biomolecules.

2. Methods

2.1. Experimental

The experiments were carried in a differentially pumped molecular beam machine and the details of the experimental setup were provided elsewhere.[32] The melting point of 26DAI molecule is ~ 93ºC and therefore, was heated to 85ºC to obtain sufficient vapour pressure required for the experiment. The sample vapours were supersonically expanded using a pulsed valve into the vacuum (10^{-6} bar) using He (2 bar) as a carrier gas. The above adiabatic expansion produces ultra-cold molecules in a collision-free environment, which allows the higher resolution studies without any interfering effects as in the case of condensed medium. The low temperature offers the benefit of simplifying spectra by predominantly populating molecules in their lowest quantum states.

A frequency-doubled tunable dye laser output, which was pumped by the second harmonic of an Nd:YAG laser, was used to electronically excite the supersonic jet cooled molecules. To get the lasing in 560-625 nm region, a mixture of rhodamine 6G (0.51 mM) and DCM (0.85 mM) dyes in methanol was used.[33] The total fluorescence of the molecule is collected by a photomultiplier tube (PMT) using laser induced fluorescence (LIF) technique. To record the single vibronic level fluorescence spectrum (SVLF), the molecules are excited at the band

origin and the resulting fluorescence emission was further dispersed using a 1.5 m spectrometer. The two-colour resonant two-photon ionization (2C-R2PI) spectrum was recorded by introducing the excitation laser at right angle to the collimated (using a skimmer) molecular beam in the detection chamber, which is equipped with a linear Time-of-flight mass spectrometer (TOFMS). A subsequent ionization laser was introduced and the resulting ions were detected using a microchannel plate (MCP) detector. Photoionization efficiency (PIE) spectrum was recorded to determine the ionization energy of the molecule. The PIE spectrum was recorded by scanning the frequency doubled visible optical parametric oscillator (OPO) wavelength. To record 2C-R2PI spectrum, ionizing laser was fixed at 240 nm.

The N-H stretching frequency of the molecule in the ground state was recorded using the FDIR spectroscopic technique, in which the scanning IR laser was introduced 5 ns prior to the excitation laser. The single Nd:YAG laser of OPO was used to pump both the excitation laser (UV laser) for the $S_1 \leftarrow S_0$ transition and the tunable IR-OPO. The optical delay of 5 ns between the excitation and the IR laser was generated by increasing the path length of the excitation laser. All the experiments were conducted using a laser power of about 0.2 mJ/pulse for UV laser and 5 mJ/pulse for IR laser with a beam size of about 2 mm. In the visible region, the bandwidth of the dye laser output was approximately 0.3 cm^{-1}. The spectrometer's resolution was 0.02 nm for the experiment with the slit width of 100 µm. The resolution of the IR-OPO and UV-VIS OPO employed for ionization is ~5 cm^{-1} and 0.1 nm, respectively.

2.2. Computational

The geometry of 26DAI in the ground and excited states were optimized using B3LYP density functional with use of the dispersion corrected density functional theory (DFT-D4) and def2-TZVPP basis set. The calculations were performed using TURBOMOLE program. The resulting structures were confirmed without any imaginary harmonic vibrational frequencies at the same level of theories. The SCF energy convergence and the optimization thresholds for changes in the energy were set to 10^{-6} E_h with the changes in the gradient at 10^{-4} E_h/a_0. The Franck-Condon simulations were carried out using the optimized S_0 and S_1 geometries. Puglisi et al.'s FC-LabWin application was used to carry out the simulations.[34] The resolution of the simulated spectrum was set at 3 cm^{-1} for the comparison with the experimental spectral bandwidth. Zero-point corrected energies of the fully optimized structures of the corresponding cationic species were used to calculate the adiabatic ionization energies.

3. Results and Discussion

3.1. $S_1 \leftarrow S_0$ transition: 2C-R2PI and LIF spectroscopic methods

The $S_1 \leftarrow S_0$ excitation spectrum of 26DAI has not been reported in the literature. The band origin of its structural isomer, 2,7-diazaindole (27DAI), was reported at 33910 cm^{-1}.[26] The $S_1 \rightarrow S_0$ electronic transition of 26DAI was expected at 33910±200 cm^{-1}. Figure 1 shows the R2PI (top) and inverted LIF (bottom) spectra of 26DAI produced under supersonic jet cooled conditions. The strongest transition in the LIF spectrum region is positioned at 33915 cm^{-1}, with additional weak transitions in both blue and red spectral regions. The mass selective R2PI spectrum (Figure 1) was recorded by monitoring the ion signal at m/z = 119. The R2PI spectrum shows a strong transition at 33915 cm^{-1} (294.855±0.005 nm), similar to that in the LIF spectrum. The band is assigned as the band origin for $S_1 \leftarrow S_0$ electronic transition. As shown in the figure, two additional bands (marked with asterisk) at 33829 (0_0^0 - 86) cm^{-1} and 33817(0_0^0 - 98) cm^{-1} were detected using both the R2PI and LIF spectroscopy. SI Figure S1 shows the LIF spectrum of 26DAI in the presence of water vapour in the pre-expansion region. The addition of water vapour increases the intensities of the bands positioned at 33829 cm^{-1} and 33817 cm^{-1}. Therefore, the marked bands are assigned to the fragmentation 26DAI-$(H_2O)_n$ complexes at the 26DAI mass channel.

The band origin of the $S_1 \leftarrow S_0$ transition of 26DAI at 33915±1 cm^{-1} is marginally red shifted than that of the 27DAI (33910 cm^{-1}).[26] However, the band origin of 26DAI is redshifted by 713 cm^{-1} and 1317 cm^{-1} from that of 7-azaindole (34628 cm^{-1}) and indole (35232 cm^{-1}), respectively.[24,25] It is worth mentioning that, in the solvation phase experiments, the λ_{max} of the absorption spectra of aqueous 26DAI and 27DAI solutions were detected at 295-300 nm region, which were redshifted by 7-10 nm from that of the aqueous 7-azaindole solution.[5,28] Therefore, the additional N-insertion resulted stabilization of the $\pi\pi^*$ state.

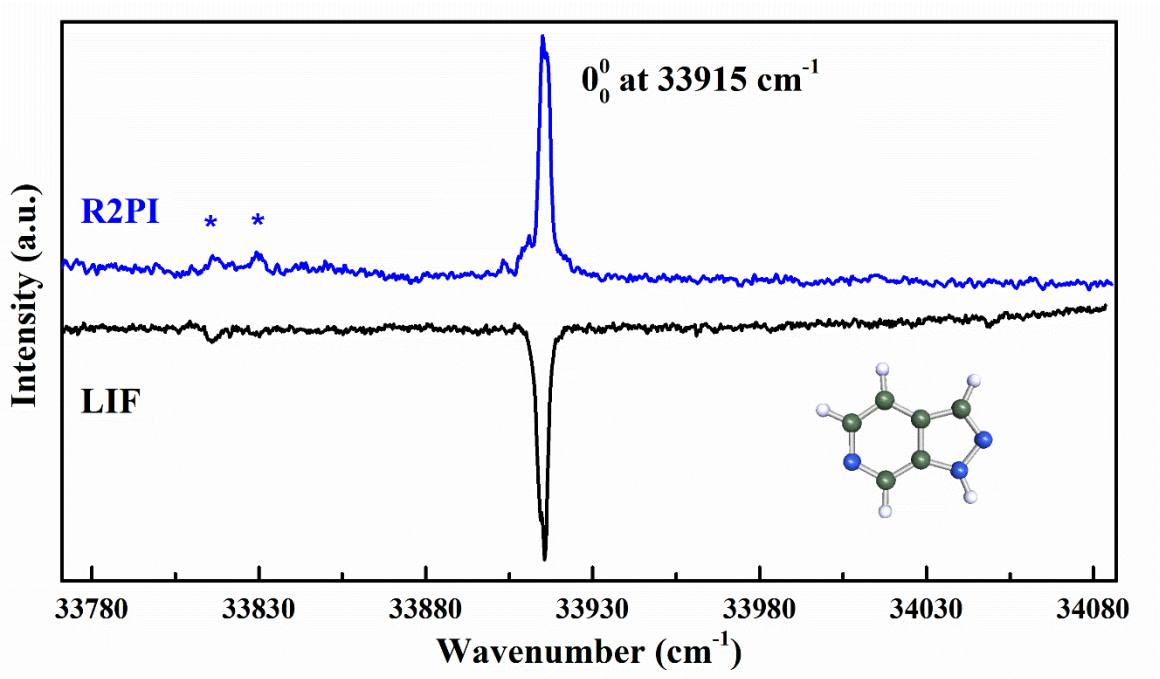

Figure 1. $S_1 \leftarrow S_0$ electronic excitation spectra of the 2,6-diazaindole are shown as the (bottom) inverted laser induced fluorescence (LIF) spectrum (black trace) and (top) two-colour resonant two-photon ionization (2C-R2PI) spectrum recorded with a 240 nm ionization laser (blue trace). The asterisk are due to the fragmentation from 26DAI-$(H_2O)_n$ at the 26DAI mass channel. The structure of the 26DAI molecule is shown at the bottom.

3.2. Single vibronic level fluorescence (SVLF) spectrum

SVLF spectrum of 2,6-DAI molecule along with its Franck-Condon simulated spectrum is shown in Figure 2. The SVLF spectrum was obtained by pumping excitation laser at $S_1 \leftarrow S_0$ transition at 33915 cm^{-1} and the resulting fluorescence was dispersed using a monochromator and the intensity of fluorescence were recorded as a function of emission wavenumbers. The ground state vibrational bands and their possible assignments based on Franck-Condon simulations are given in the Table 1.

The ground state vibrational modes are detected till 2500 cm^{-1}. The majority of the modes are symmetric which can be seen in the Table 1. The lower energy totally symmetric modes at 427 (ν_{25}"), 554 (ν_{24}"), 643 (ν_{23}") cm^{-1} are in good agreement with the calculated ones at 402 (390), 560 (542), 643 (618) cm^{-1}, respectively, at B3LYP-D4/def2-TZVPP level of theory (values in parentheses are scaled by a factor of 0.968). The higher energy modes are observed at 773 (ν_{22}"), 850 (ν_{21}"), 935 (ν_{20}") and 1039 (ν_{19}") cm^{-1}, which were predicted at 779, 881, 929 and 1024 cm^{-1} (Table 1) at B3LYP-D4/def2-TZVPP level of theory. As shown in Figure 2, the

SVLF spectroscopy gives the Franck Condon active vibrational modes in the ground states from the vibrationless excited state. The simulated spectrum has reproduced the positions and intensities of the totally symmetric modes better than the asymmetric and combination modes. The above provide us an opportunity to understand the accuracy of the calculated frequencies in the ground states at different computational methods.

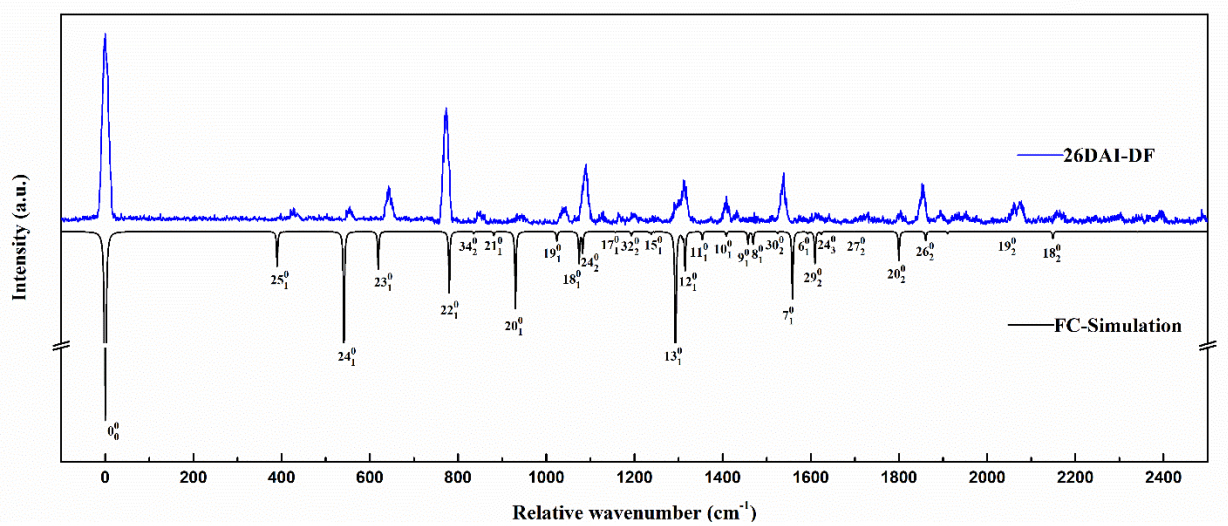

Figure 2. The single vibronic level fluorescence (SVLF) spectrum of 2,6-DAI molecule (blue trace) recorded by exciting at the origin band positioned at 33915 cm^{-1}. The inverted Franck-Condon simulated spectrum of the $S_0 \leftarrow S_1$ transition with assignments (black trace).

Table 1. The experimental vibrational frequencies along with their calculated vibrational frequencies in the ground state are shown in cm^{-1}. The possible assignments based on the FCF simulated spectrum are given. The calculated frequencies are scaled using 0.968 and 0.955 at B3LYP-D4 and MP2 levels of theories, respectively, as obtained from the correlation fit shown in Figure 3.

Bands	ν''_{expt}	ν''_{calc} B3LYP-D4	ν''_{calc} MP2	Assignment
33915	0	-	-	0_0^0
34342	427	390	377	25_1^0
34469	554	542	530	24_1^0
34558	643	618	602	23_1^0
34687	773	779	763	22_1^0
34769	850	881	874	21_1^0
34847	935	929	916	20_1^0
34949	1039	1024	1002	19_1^0
35002	1091	1075	1088	18_1^0
35044	1128	1081	1058	24_2^0

35080	1166	1156	1152	17_1^0
35109	1196	1193	--	32_2^0
35162	1245	1239	--	15_1^0
35229	1312	1317	1333	12_1^0
35291	1372	1356	1381	11_1^0
35324	1410	1407	1400	10_1^0
35349	1433	1459	1444	9_1^0
35387	1472	1471	1479	8_1^0
35453	1514	1525	--	30_2^0
35489	1539	1558	1556	7_1^0
35534	1574	1594	1607	6_1^0
35645	1616	1624	--	24_3^0
35717	1803	1801	1832	20_2^0
35767	1852	1860	--	26_2^0
35811	2070	2049	2007	19_2^0
35865	2156	2150	2181	18_2^0

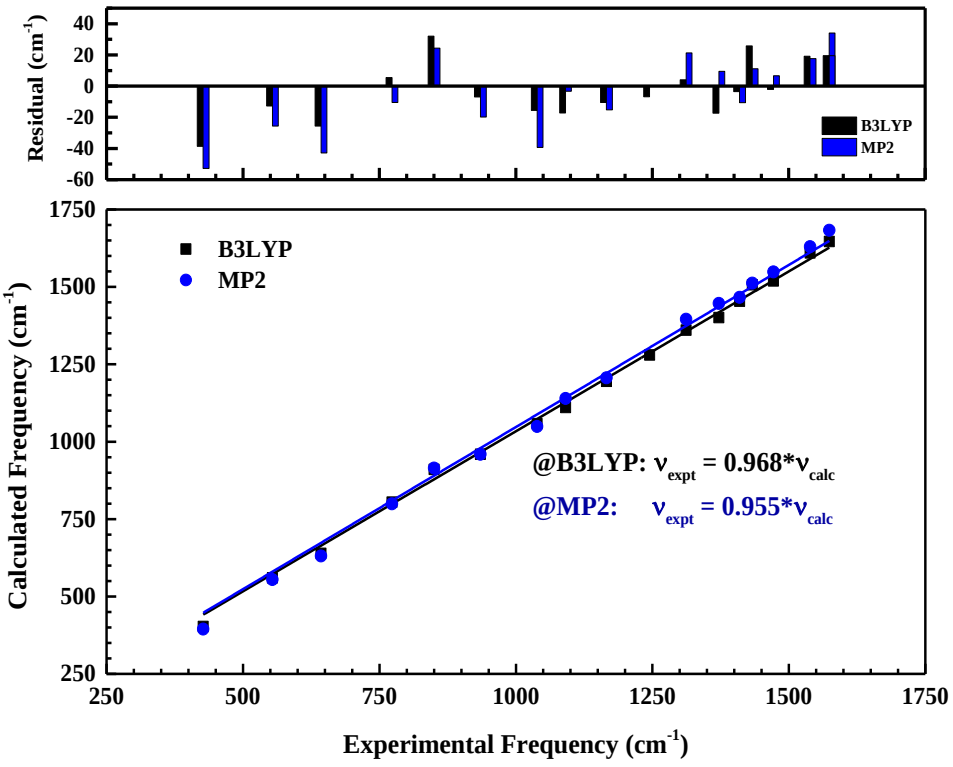

Figure 3. The correlation between experimental and calculated frequencies obtained at B3LYP-D4/def2-TZVPP and MP2/cc-pVDZ level of theories. The correlation factors are 0.968 and 0.955 at the respective methods. The associated residuals of the fits are shown at the top.

Figure 3 shows the correlation between experimental and calculated frequencies obtained using two methods, B3LYP-D4/def2-TZVPP and MP2/cc-pVDZ. The fits are shown with the respective linear fit factors of 0.968 and 0.955. The above factors are marginally lower to that obtained in the case of 27DAI molecule (0.976 at B3LYP-D4 and 0.967 at MP2/cc-pVDZ). Table 1 lists the experimental bands, and the assignments based on the calculated Franck Condon factors. The calculated frequencies are given with a factor of 0.968 (at B3LYP) and 0.955 (at MP2) obtained by fitting the experimental and calculated totally symmetric modes.

3.3. Fluorescence dip infrared (FDIR) spectroscopy

The N-H stretching frequency of 26DAI were recorded by FDIR spectroscopy and is shown in Figure 4. In this, the excitation laser was fixed at the band origin of 26DAI molecule at 33915 cm^{-1}. The scanning IR-OPO laser was introduced 5 ns prior to the excitation laser and the resultant dip was monitored as a function of the IR frequency. As shown in Figure 4, the FDIR spectrum shows an intense peak at 3524±5 cm^{-1}. The calculated ground state N-H stretching frequency of 26DAI at B3LYP-D4/def2-TZVPP level of theory was found as 3672 cm^{-1}. Using the recommended scaling factor of 0.965 from the CCCBDB, NIST, the scaled calculated frequency appears at 3544 cm^{-1}, which has shown good correlation with the experimental value. The ground state N-H stretching frequency of 2,7-DAI (3523 cm^{-1}) was nearly same as that of the current value at 3524 cm^{-1}.

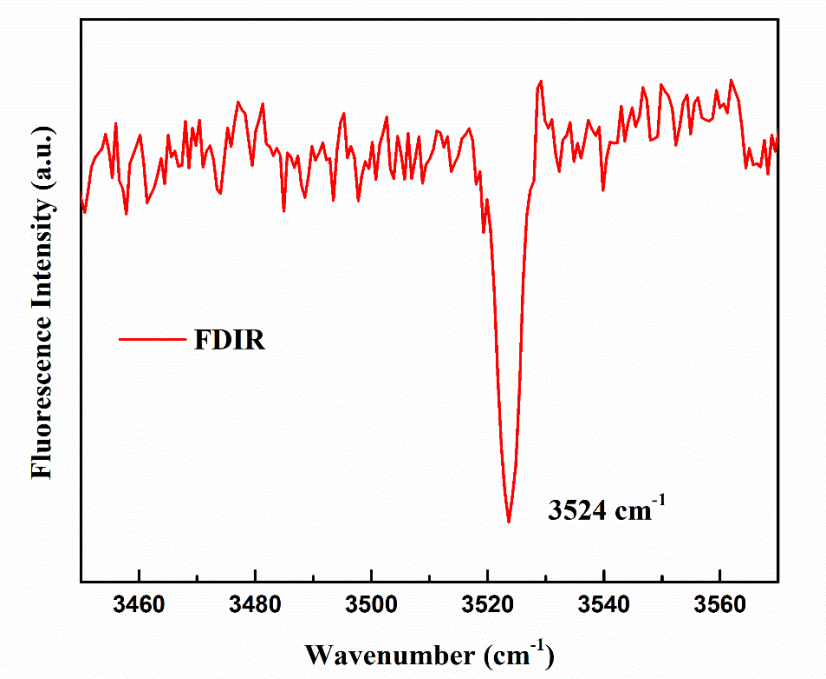

Figure 4. FDIR spectrum of 26DAI where the excitation laser was fixed at the $S_1 \leftarrow S_0$ transition at 33915cm^{-1}.

3.4. Photoionization efficiency spectroscopy

The photoionization efficiency (PIE) is a powerful technique to investigate the photo ionization energy, and thus relevant to study the stability of organic molecules exposed to solar radiation. Additionally, for the present study, the ionization energy is crucial to employ the ionization laser to record electronic spectrum of 26DAI using R2PI spectroscopy. The R2PI schemes using (1+1) with origin band at 33915 cm^{-1} and (1+1') scheme with ionization photon of 266 nm (1' at 37594 cm^{-1}) failed to produce any signal. The above confirmed that the molecule does not ionize at 67830 - 71509 cm^{-1} energy region, like the structural isomer 27DAI. Therefore, to determine the ionization energy of the molecule photoionization efficiency spectrum was recorded, by fixing the excitation laser at 33915 cm^{-1}. A scanning second UV laser from OPO (band width of 5 cm^{-1}) was introduced ~ 0-3 ns after the excitation laser. The recorded PIE spectrum of 2,6-DAI molecule is shown in Figure 5, with the x-axis representing total energy of excitation and ionization photons. The ionization energy was selected as the intersection point of linear fits of the initial rise in ion signal and the base line. The experimental ionization energy of 26DAI is thus measured as 71866 cm^{-1} which is marginally lower (87 cm^{-1}) than that of 27DAI (71953 cm^{-1}). The above measured ionization energy of 26DAI is significantly higher than the already reported values for 7-azaindole (65412 cm^{-1}) and indole (62589 cm^{-1}). This suggests that the N-rich chromophores have higher photostability.

Moreover, as shown in SI Scheme S1, the $S_1 \leftarrow S_0$ origin of indole, 7AI, 27DAI and 26DAI molecules fall in the UVB region 289±6 nm. Indole and 7AI molecules can be ionised by photons of energy ranging from 365±1 nm (UVA) to the excitation energy (UVB) of the molecules. However, for 27DAI and 26DAI molecules, the energy of ionizing photons ranges at 263±1 nm or lower, falling in the UVC region. Since UVC photons, in comparison to UVA and UVB photons, can barely penetrate the earth's atmosphere, the insertion of N-atom in 26DAI and 27DAI molecules can lower the risk of photodamage as compared to indole and 7AI molecules.

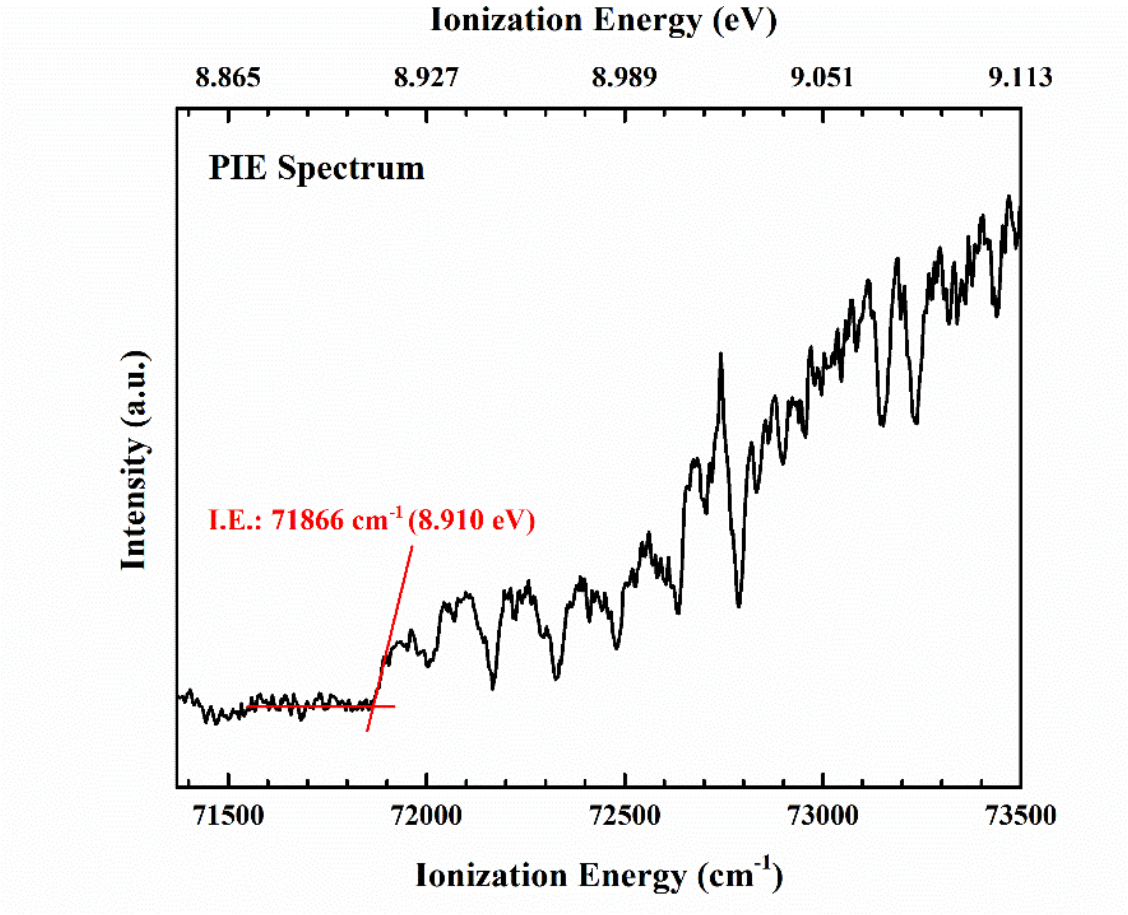

Figure 4. The photoionization efficiency (PIE) spectrum of 2,6-DAI molecule was recorded by keeping the excitation laser at the band origin at 33915 cm^{-1}.

Conclusion:

In this study, 26DAI molecule was experimentally investigated in the gas phase by using different laser spectroscopic techniques. Laser induced fluorescence (LIF) and two-colour resonant two-photon ionization (2C-R2PI) spectroscopic techniques were performed to record $S_1 \leftarrow S_0$ electronic transition of 26DAI molecule. The $S_1 \leftarrow S_0$ band origin was observed at 33915 cm^{-1} which is redshifted by 713 cm^{-1} and 1317 cm^{-1} from that of 7-azaindole and indole molecules. In the SVLF spectrum the Franck-Condon active vibrational modes in the ground state are found till 2500 cm^{-1}. Furthermore, to understand the ground state properties of the molecule, the experimental vibrational frequencies were compared to the calculated ones at two different levels of theory. The calculated frequencies at B3LYP-D4/def2-TZVPP level of theory showed better results for the experimentally observed symmetric modes of the molecule in the ground state.

The N–H stretching frequency of 26DAI molecule in the ground state was determined by recording fluorescence-dip infrared (FDIR) spectrum. The ground state frequency was obtained at 3524 cm^{-1} which was found to be in good correlation with the calculated value at B3LYP-D4/def2-TZVPP level of theory. To determine I.E. of the molecule, photoionization efficiency spectrum was recorded which was obtained as 71866 cm^{-1}. The above value is marginally lower than the I.E. of 27DAI (71953 cm^{-1}), however it is significantly higher than the reported value of I.E. of 7AI (65412 cm^{-1}) and indole (62589 cm^{-1}) molecules. The higher energy of ionizing photons, required for N-rich biomolecules, falls in UVC region. Thus, N-rich chromophores have shown higher resistivity towards photodamage compared to 7AI and indole. The current study implies that the gradual N-insertion at selective positions can lead to the higher photo-stability of N-bearing biorelevant molecule.

Conflicts of interest

There are no conflicts to declare.

Acknowledgements

This work has been supported by the Department of Chemistry, IIT Hyderabad and MHRD, the Government of India. BK thanks UGC for the research fellowship. SB thanks MoE for the research fellowship. SM expresses sincere gratitude to Prof. Samuel Leutwyler, the University of Bern, for his generous instrumentation aid to IITH for the experimental set-up. SM thanks SERB, DST Government of India (Grant no. CRG/2019/003335) for funding.

References:

[1] Y. Cben, R.L. Rich, F. Cai, J.W. Petrich', Fluorescent Species of 7-Azaindole and 7-Azatryptophan in Water, J Phys Chem 97 (1993) 1770-1780. https://doi.org/10.1021/j100111a011.

[2] M.T. Cash, P.R. Schreiner, R.S. Phillips, Excited state tautomerization of azaindole, Org Biomol Chem 3 (2005) 3701–3706. https://doi.org/10.1039/b506652b

[3] R.J. Reiter, D.-X. Tan, J. Cabrera, D.D.' Arpa, R.M. Sainz, J.C. Mayo, S. Ramos, The Oxidant/Antioxidant Network: Role of Melatonin, Neurosignals 8 (1999) 56-63. http://BioMedNet.com/karger.

[4] J. Onvlee, S. Trippel, J. Küpper, Ultrafast light-induced dynamics in the microsolvated biomolecular indole chromophore with water, Nat Commun 13 (2022) 7462. https://doi.org/10.1038/s41467-022-33901-w.

[5] J.Y. Shen, W.C. Chao, C. Liu, H.A. Pan, H.C. Yang, C.L. Chen, Y.K. Lan, L.J. Lin, J.S. Wang, J.F. Lu, S. Chun-Wei Chou, K.C. Tang, P.T. Chou, Probing water micro-solvation in proteins by water catalysed proton-transfer tautomerism, Nat Commun 4 (2013) 2611. https://doi.org/10.1038/ncomms3611.

[6] A. Echalier, K. Bettayeb, Y. Ferandin, O. Lozach, M. Clément, A. Valette, F. Liger, B. Marquet, J.C. Morris, J.A. Endicott, B. Joseph, L. Meijer, Meriolins (3-(pyrimidin-4-yl)-7-azaindoles): Synthesis, kinase inhibitory activity, cellular effects, and structure of a CDK2/Cyclin A/meriolin complex, J Med Chem 51 (2008) 737–751. https://doi.org/10.1021/jm700940h.

[7] S.R. Walker, E.J. Carter, B.C. Huff, J.C. Morris, Variolins and related alkaloids, Chem Rev 109 (2009) 3080–3098. https://doi.org/10.1021/cr900032s.

[8] K.T. Homan, J.J.G. Tesmer, Molecular basis for small molecule inhibition of G protein-coupled receptor kinases, ACS Chem Biol 10 (2015) 246–256. https://doi.org/10.1021/cb5003976.

[9] J.Y. Mérour, F. Buron, K. Plé, P. Bonnet, S. Routier, The azaindole framework in the design of kinase inhibitors, Molecules 19 (2014) 19935–19979. https://doi.org/10.3390/molecules191219935.

[10] S. Sharma, R. Rao, S.M. Reeve, G.A. Phelps, N. Bharatham, N. Katagihallimath, V. Ramachandran, S. Raveendran, M. Sarma, A. Nath, T. Thomas, D. Manickam, S. Nagaraj, V. Balasubramanian, R.E. Lee, S. Hameed P, S. Datta, Azaindole Based Potentiator of Antibiotics against Gram-Negative Bacteria, ACS Infect Dis 7 (2021) 3009–3024. https://doi.org/10.1021/acsinfecdis.1c00171.

[11] A. Zamora, V. Rodríguez, N. Cutillas, G.S. Yellol, A. Espinosa, K.G. Samper, M. Capdevila, Ò. Palacios, J. Ruiz, New steroidal 7-azaindole platinum(II) antitumor complexes, J Inorg Biochem 128 (2013) 48–56. https://doi.org/10.1016/j.jinorgbio.2013.07.010.

[12] S. Bin Zhao, S. Wang, Luminescence and reactivity of 7-azaindole derivatives and complexes, Chem Soc Rev 39 (2010) 3142–3156. https://doi.org/10.1039/c001897j.

[13] E. Wong, J. Li, C. Seward, S. Wang, Cu(i) and Ag(i) complexes of 7-azaindolyl and 2,2′-dipyridylamino substituted 1,3,5-triazine and benzene: The central core impact on structure, solution dynamics and fluorescence of the complexes, Dalton Trans 10 (2009) 1776–1785. https://doi.org/10.1039/b814393e.

[14] A. Domínguez-Martín, M. del P. Brandi-Blanco, A. Matilla-Hernández, H. El Bakkali, V.M. Nurchi, J.M. González-Pérez, A. Castiñeiras, J. Niclós-Gutiérrez, Unravelling the versatile metal binding modes of adenine: Looking at the molecular recognition patterns of deaza- and aza-adenines in mixed ligand metal complexes, Coord Chem Rev 257 (2013) 2814–2838. https://doi.org/10.1016/j.ccr.2013.03.029.

[15] B. Morzyk-Ociepa, K. Szmigiel, R. Petrus, I. Turowska-Tyrk, D. Michalska, A novel coordination polymer of 7-azaindole-3-carboxylic acid with sodium ions: crystal and molecular structures, vibrational spectra and DFT calculations, J Mol Struct 1144 (2017) 338–346. https://doi.org/10.1016/j.molstruc.2017.05.059.

[16] M. Négrerie, F. Gai, J.-C. Lambry, J.-L. Martin, J.W. Petrich, Photoionization and Dynamic Solvation of the Excited States of 7-Azaindole, J Phys Chem 97 (1993) 5046-5049. https://pubs.acs.org/sharingguidelines.

[17] S. Takeuchi, T. Tahara, The answer to concerted versus step-wise controversy for the double proton transfer mechanism of 7-azaindole dimer in solution, Proc. Natl. Acad. Sci 104 (2007) 5285-5290. https://doi.org/10.1073/pnas.0610141104.

[18] W.T. Hsieh, C.C. Hsieh, C.H. Lai, Y.M. Cheng, M.L. Ho, K.K. Wang, G.H. Lee, P.T. Chou, Excited-state double proton transfer in model base pairs: The stepwise reaction on the heterodimer of 7-azaindole analogues, Chem Phys Chem 9 (2008) 293–299. https://doi.org/10.1002/cphc.200700578.

[19] H. Ishikawa, H. Yabuguchi, Y. Yamada, A. Fujihara, K. Fuke, Infrared spectroscopy of jet-cooled tautomeric Dimer of 7-Azaindole: a Model system for the ground-State double proton transfer reaction, J Phys Chem A 114 (2010) 3199–3206. https://doi.org/10.1021/jp909337w.

[20] R. Crespo-Otero, N. Kungwan, M. Barbatti, Stepwise double excited-state proton transfer is not possible in 7-azaindole dimer, Chem Sci 6 (2015) 5762–5767. https://doi.org/10.1039/c5sc01902h.

[21] O.-H. Kwon, A.H. Zewail, Double proton transfer dynamics of model DNA base pairs in the condensed phase, Proc. Natl. Acad. Sci 104 (2007) 8703-8708. https://doi.org/10.1073/pnas.0702944104.

[22] A. V Smirnov, + D S English, R.L. Rich, J. Lane, L. Teyton, | A W Schwabacher, ⊥ S Luo, R.W. Thornburg, J.W. Petrich, Photophysics and Biological Applications of 7-Azaindole and Its Analogs, J Phys Chem B 101 (1996) 2758-2769. https://pubs.acs.org/sharingguidelines.

[23] K. Sakota, H. Sekiya, Excited-state double-proton transfer in the 7-azaindole dimer in the gas phase. 1. Evidence of complete localization in the lowest excited electronic state of asymmetric isotopomers, J Phys Chem A 109 (2005) 2718–2721. https://doi.org/10.1021/jp045773e.

[24] J.L. Lin, W.B. Tzeng, Mass analyzed threshold ionization spectroscopy of 7-azaindole cation, Chem Phys Lett 380 (2003) 503–511. https://doi.org/10.1016/j.cplett.2003.09.063.

[25] J. Hager, M. Ivanco, M. A. Smith and S. C. Wallace, Solvation effects in jet-cooled van der Waals clusters: Two-color treshold photoionization spectroscopy of indole, indole-argon, indole-methane, indole-water and indole-methanol, Chem Phys Lett 113 (1985) 503-507. https://doi.org/10.1016/0009-2614(85)80090-7.

[26] S. Baweja, B. Kalal, S. Maity, Laser spectroscopic characterization of supersonic jet cooled 2,7-diazaindole, Phys Chem Chem Phys 25 (2023) 26679–26691. https://doi.org/10.1039/d3cp03010e.

[27] J.A. Noble, E. Marceca, C. Dedonder, W. Phasayavan, G. Féraud, B. Inceesungvorn, C. Jouvet, Influence of the N atom position on the excited state photodynamics of protonated azaindole, Phys Chem Chem Phys 22 (2020) 27280–27289. https://doi.org/10.1039/d0cp03608k.

[28] K.Y. Chung, Y.H. Chen, Y.T. Chen, Y.H. Hsu, J.Y. Shen, C.L. Chen, Y.A. Chen, P.T. Chou, The Excited-State Triple Proton Transfer Reaction of 2,6-Diazaindoles and 2,6-Diazatryptophan in Aqueous Solution, J Am Chem Soc 139 (2017) 6396–6402. https://doi.org/10.1021/jacs.7b01672.

[29] S. Baweja, B. Kalal, P. Kumar Mitra, S. Maity, Competing Excited-State Hydrogen and Proton-Transfer Processes in 6-Azaindole-$S_{3,4}$ and 2,6-Diazaindole-$S_{3,4}$ Clusters (S=H_2O, NH_3), Chem Phys Chem 24 (2023) e202300270. https://doi.org/10.1002/cphc.202300270.

[30] Z. Tang, Y. Qi, Y. Wang, P. Zhou, J. Tian, X. Fei, Excited-State Proton Transfer Mechanism of 2,6-Diazaindoles·(H2O)n (n = 2-4) Clusters, J Phys Chem B 122 (2018) 3988–3995. https://doi.org/10.1021/acs.jpcb.7b10207.

[31] J.D. Huang, H. Ma, The mechanism of the excited-state multiple proton transfer reaction for 3-Me-2,6-diazaindole in aqueous solution, Org Chem Front 5 (2018) 2749–2753. https://doi.org/10.1039/c8qo00628h.

[32] S. Maity, R. Knochenmuss, C. Holzer, G. Féraud, J. Frey, W. Klopper, S. Leutwyler, Accurate dissociation energies of two isomers of the 1-naphtho⩽cyclopropane complex, J Chem Phys 145 (2016) 164304. https://doi.org/10.1063/1.4965821.

[33] S. Sinha, A.K. Ray, S. Kundu, T.B. Pal, S.K.S. Nair, K. Dasgupta, Spectral characteristics of a binary dye-mixture laser, App Opt 41 (2002) 7006-7011. https://doi.org/10.1364/AO.41.007006.

[34] I. Pugliesi, K. Müller-Dethlefs, The use of multidimensional Franck-Condon simulations to assess model chemistries: A case study on phenol, J Phys Chem A 110 (2006) 4657–4667. https://doi.org/10.1021/jp058226h.